JCI The Journal of Clinical Investigation

Imiquimod clears tumors in mice independent of adaptive immunity by converting pDCs into tumor-killing effector cells

Barbara Drobits, … , Marco Colonna, Maria Sibilia

J Clin Invest. 2012;122(2):575-585. https://doi.org/10.1172/JCI61034.

Research Article

Imiquimod is a synthetic compound with antitumor properties; a 5% cream formulation is successfully used to treat skin tumors. The antitumor effect of imiquimod is multifactorial, although its ability to modulate immune responses by triggering TLR7/8 is thought to be key. Among the immune cells suggested to be involved are plasmacytoid DCs (pDCs). However, a direct contribution of pDCs to tumor killing in vivo and the mechanism of their recruitment to imiquimod-treated sites have never been demonstrated. Using a mouse model of melanoma, we have now demonstrated that pDCs can directly clear tumors without the need for the adaptive immune system. Topical imiquimod treatment led to TLR7-dependent and IFN-α/β receptor 1–dependent (IFNAR1-dependent) upregulation of expression of the chemokine CCL2 in mast cells. This was essential to induce skin inflammation and for the recruitment of pDCs to the skin. The recruited pDCs were $CD8\alpha^+$ and induced tumor regression in a TLR7/MyD88- and IFNAR1-dependent manner. Lack of TLR7 and IFNAR1 or depletion of pDCs or $CD8\alpha^+$ cells from tumor-bearing mice completely abolished the effect of imiquimod. TLR7 was essential for imiquimod-stimulated pDCs to produce IFN-α/β, which led to TRAIL and granzyme B secretion by pDCs via IFNAR1 signaling. Blocking these cytolytic molecules impaired pDC-mediated tumor killing. Our results demonstrate that imiquimod treatment leads to CCL2-dependent recruitment of pDCs and their transformation into […]

Imiquimod clears tumors in mice independent of adaptive immunity by converting pDCs into tumor-killing effector cells

Barbara Drobits,[1] Martin Holcmann,[1] Nicole Amberg,[1] Melissa Swiecki,[2] Roland Grundtner,[1] Martina Hammer,[1] Marco Colonna,[2] and Maria Sibilia[1]

[1]Institute for Cancer Research, Department of Medicine I, Comprehensive Cancer Center, Medical University of Vienna, Vienna, Austria.
[2]Department of Pathology and Immunology, Washington University School of Medicine, St. Louis, Missouri, USA.

Imiquimod is a synthetic compound with antitumor properties; a 5% cream formulation is successfully used to treat skin tumors. The antitumor effect of imiquimod is multifactorial, although its ability to modulate immune responses by triggering TLR7/8 is thought to be key. Among the immune cells suggested to be involved are plasmacytoid DCs (pDCs). However, a direct contribution of pDCs to tumor killing in vivo and the mechanism of their recruitment to imiquimod-treated sites have never been demonstrated. Using a mouse model of melanoma, we have now demonstrated that pDCs can directly clear tumors without the need for the adaptive immune system. Topical imiquimod treatment led to TLR7-dependent and IFN-α/β receptor 1–dependent (IFNAR1-dependent) upregulation of expression of the chemokine CCL2 in mast cells. This was essential to induce skin inflammation and for the recruitment of pDCs to the skin. The recruited pDCs were CD8α$^+$ and induced tumor regression in a TLR7/MyD88- and IFNAR1-dependent manner. Lack of TLR7 and IFNAR1 or depletion of pDCs or CD8α$^+$ cells from tumor-bearing mice completely abolished the effect of imiquimod. TLR7 was essential for imiquimod-stimulated pDCs to produce IFN-α/β, which led to TRAIL and granzyme B secretion by pDCs via IFNAR1 signaling. Blocking these cytolytic molecules impaired pDC-mediated tumor killing. Our results demonstrate that imiquimod treatment leads to CCL2-dependent recruitment of pDCs and their transformation into a subset of killer DCs able to directly eliminate tumor cells.

Introduction

Imiquimod (Imi) belongs to the group of imidazoquinolines and has been shown to induce antiviral and antitumor immune responses (1). Aldara, a 5% cream formulation of Imi, has been approved for treatment of superficial basal cell carcinoma, squamous cell carcinoma, lentigo maligna, and actinic keratoses (1). In addition to its antiangiogenic (2) and proapoptotic activity (3), Imi has been shown to regulate the function of immune cells by triggering TLR7 and TLR8 (4), both of which have been identified as receptors for single-stranded RNA (5). There are also indications for TLR-independent effects of Imi that are induced by the adenosine receptor (6) or the inflammasome (7).

TLRs are pattern recognition receptors involved in sensing foreign antigens. TLR triggering leads to the production of proinflammatory cytokines necessary for initiating innate and boosting adaptive immune responses, thereby facilitating elimination of pathogens and tumor cells (8). A central role at the interface of innate and adaptive immunity is played by DCs, which are professional antigen-presenting cells. Murine plasmacytoid DCs (pDCs) constitutively express high levels of TLR7 and TLR9 (9). These receptors signal via the adapter molecule myeloid differentiation primary response protein 88 (MyD88), thereby activating NF-κB, IRF-7, and the MAPK pathway, leading to secretion of cytokines and chemokines, such as IL-1, TNF-α, IL-6, IL-8, and especially type I IFNs (IFN-α/β) (5, 8, 10, 11). Several studies have demonstrated that IFNs are able to induce apoptosis on malignant cells, either by directly exerting cytotoxic effects or by enhancing the expression of death-inducing molecules, such as TNF-related apoptosis-inducing ligand (TRAIL) and FasL (12–14). Notably, human pDCs were reported to express TRAIL and FasL or to release granzyme B upon TLR7/8 stimulation by viruses or synthetic ligands (15–17). We and others have shown that topical application of Imi induces epidermal thickening and dermal inflammation with infiltration of immune cells and production of IFN-α and TNF-α (18, 19). Imi treatment leads to emigration of Langerhans cells from the epidermis and massive recruitment of pDCs into the dermis, in which they are present at very low numbers in normal skin (18, 19). Chemoattractants, like CXCL9-12, CXCL4, CCL2, and CCL5, whose cognate receptors are highly expressed on pDCs, may facilitate their recruitment (20, 21). pDCs have been described to be present in increased numbers in different tumors upon activation with various TLR agonists (17, 18, 22, 23). Systemic administration of CpG induced an influx of pDCs into lung tumors, which led to tumor progression by the recruitment of regulatory T cells (23). On the contrary, CpG-activated pDCs were found to induce NK cell–dependent tumor regression in a mouse melanoma model (22). We could also demonstrate that treatment of intradermally induced melanomas with Imi led to tumor regression and that treatment success correlated with increased numbers of infiltrating pDCs in the tumors (18).

From these results it is clear that the precise function of pDCs in modulating immune responses against tumors is still controversial and remains to be determined. So far it has never been shown whether infiltrating pDCs directly contribute to tumor killing and whether TLR7/8 stimulation is required for the antitumor

Authorship note: Barbara Drobits and Martin Holcmann contributed equally to this work.

Conflict of interest: The authors have declared that no conflict of interest exists.

Citation for this article: *J Clin Invest.* 2012;122(2):575–585. doi:10.1172/JCI61034.

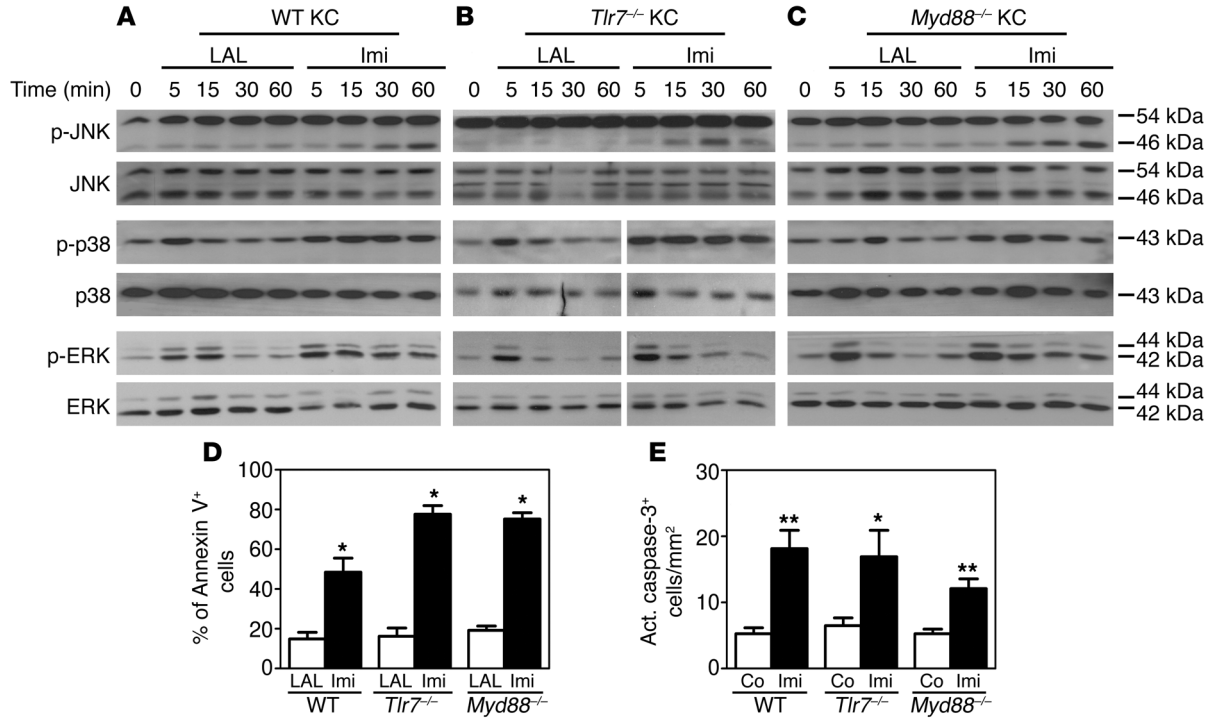

Figure 1

TLR7/MyD88-independent effects of Imi in the skin. Western blot analysis of primary keratinocytes (KCs) isolated from (**A**) C57BL/6 (WT), (**B**) *Tlr7*$^{-/-}$, and (**C**) *Myd88*$^{-/-}$ mice treated with 12 μg/ml Imi or LAL reagent water (control) for the indicated time points. Results are representative of at least 3 independent batches. White lines indicate that samples were run on the same gel but were noncontiguous. (**D**) Flow cytometric analysis showing annexin V$^+$ cells in primary keratinocyte cultures stimulated with Imi (12 μg/ml) or LAL water for 40 hours (n = 3–4 per group). (**E**) Apoptosis was measured by active (act.) caspase-3 staining of epidermal sheets from ears of WT, *Tlr7*$^{-/-}$, and *Myd88*$^{-/-}$ mice treated topically with Imi for 7 days or left untreated (Co). Caspase-3$^+$ cells were counted in 10 randomly chosen fields of at least 3 independent samples. *P < 0.05, **P < 0.005.

activity of Imi. Moreover, it is unclear by which trigger pDCs are recruited to the skin upon Imi treatment. In the present study, we show that CCL2, produced after Imi treatment by mast cells in the dermis, is responsible for recruiting pDCs to the skin. Furthermore, we demonstrate that mice lacking pDCs are not able to clear tumors after Imi treatment and unravel the mechanism by which TLR7/MyD88 as well as IFN-α/β receptor 1 (IFNAR1) signaling on pDCs is required for the antitumor effect of Imi. This study demonstrates that Imi can transform pDCs into a subset of DCs capable of directly killing tumors independent of the adaptive immune system.

Results

Effects of Imi in the skin. The epidermis is the site of first contact with topically applied Imi. Since pDCs are present only in low numbers in the skin (18), we wanted to investigate the early effects induced by Imi and identify the skin-resident cell type first responding to the drug. Therefore, we analyzed TLR expression in skin cell populations and examined whether their expression level was modulated by Imi treatment. Whereas TLR3, TLR4, TLR5, and TLR9 were expressed by various skin cells, no expression of TLR7 or TLR8 was observed (Supplemental Figure 1A; supplemental material available online with this article; doi:10.1172/JCI61034DS1). Although cultured primary keratinocytes lacked TLR7/8 expression, stimulation with Imi resulted in activation of JNK1, p38, and ERK (Figure 1A), whereas the NF-κB pathway was not affected (data not shown). Similar results were obtained with *Tlr7*$^{-/-}$ and *Myd88*$^{-/-}$ keratinocytes, indicating that Imi was acting independently of TLR7 signaling (Figure 1, B and C). Imi treatment induced cell death in cultured keratinocytes independent of the presence of TLR7 or MyD88 (Figure 1D). The proapoptotic effects of Imi were also observed in vivo in Imi-treated ears of WT, *Tlr7*$^{-/-}$, and *Myd88*$^{-/-}$ mice (Figure 1E). In contrast, Imi treatment neither activated the MAPK pathway nor induced apoptosis in WT, *Tlr7*$^{-/-}$, or *Myd88*$^{-/-}$ dermal cells (data not shown). These results demonstrate that topical Imi application leads to TLR7/MyD88-independent signaling and apoptosis in the epidermis.

Long-term treatment with Imi induces skin inflammation and secretion of inflammatory cytokines (18, 19). We were interested in identifying the factors produced by skin resident cells early after Imi application and therefore analyzed their production in the first hours after treatment. After 24 hours, cytokines like IL-6, TNF-α, CCL2, and IL-1β were not increased in keratinocytes and epidermis (Figure 2A and Supplemental Figure 1B). Similarly, neither IL-6 nor IL-1β or TNF-α were substantially increased in the dermis, suggesting that the induction of these factors occurs later as a result of inflammation and is possibly mediated by infiltrating immune cells (Figure 2B). CCL2 levels were already significantly increased 24 hours after Imi stimulation in the dermis of WT mice but not in that of *Tlr7*$^{-/-}$ or *Myd88*$^{-/-}$ mice (Figure 2C). Mast cells are resident in the skin and known to express TLR7 (24). When stimulated with Imi, mast cells released significantly increased amounts of CCL2 (Figure 2D). To investigate whether the increased CCL2 levels were responsible for pDC recruitment, mice lacking CCL2 were treated with Imi. Interestingly, pDC numbers were not increased in the

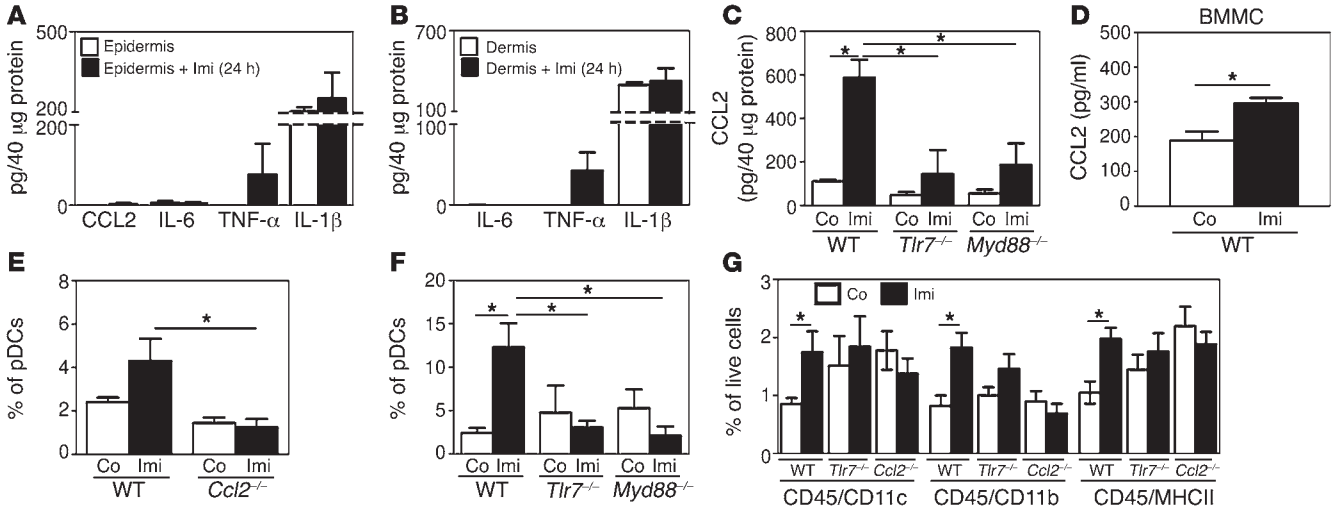

Figure 2

TLR7/MyD88-dependent effects of Imi in the skin. (**A**–**C**) Mouse back skin was treated topically for 24 hours with Imi or left untreated. IL-1β, IL-6, TNF-α, or CCL2 levels were measured in protein lysates of (**A**) epidermis and (**B** and **C**) dermis by ELISA. (**D**) BM-derived mast cells (BMMCs) were stimulated with Imi (12 μg/ml) for 20 hours, and CCL2 was measured in supernatants by ELISA. (**E** and **F**) Histograms showing the percentage of pDCs (**E**, B220$^+$Ly6C$^+$CD11b$^-$; **F**, mPDCA1$^+$B220$^+$Gr-1$^+$) among total DCs (CD45$^+$CD11c$^+$) in the dermis of (**E**) WT and *Ccl2*$^{-/-}$ and (**F**) *Tlr7*$^{-/-}$ and *Myd88*$^{-/-}$ mice after 7 days of topical Imi treatment. (**G**) Graph depicting the percentage of infiltrating immune cells in the dermis of mice after 7 days of topical Imi treatment. *$P < 0.05$.

dermis of Imi-treated CCL2-deficient mice, demonstrating that CCL2 is responsible for pDC recruitment (Figure 2E). The finding, that CCL2 expression was dependent on TLR7 and MyD88 led us to investigate whether this applied also for pDC accumulation. After Imi treatment, increased numbers of pDCs could be observed in the dermis of WT mice but not in that of mice lacking TLR7 or MyD88 (Figure 2F and Supplemental Figure 1C). Comparable to CCL2-deficient mice, Imi-induced epidermal thickening and dermal inflammation were not detectable in the skin of *Tlr7*$^{-/-}$ or *Myd88*$^{-/-}$ mice (Supplemental Figure 1D and data not

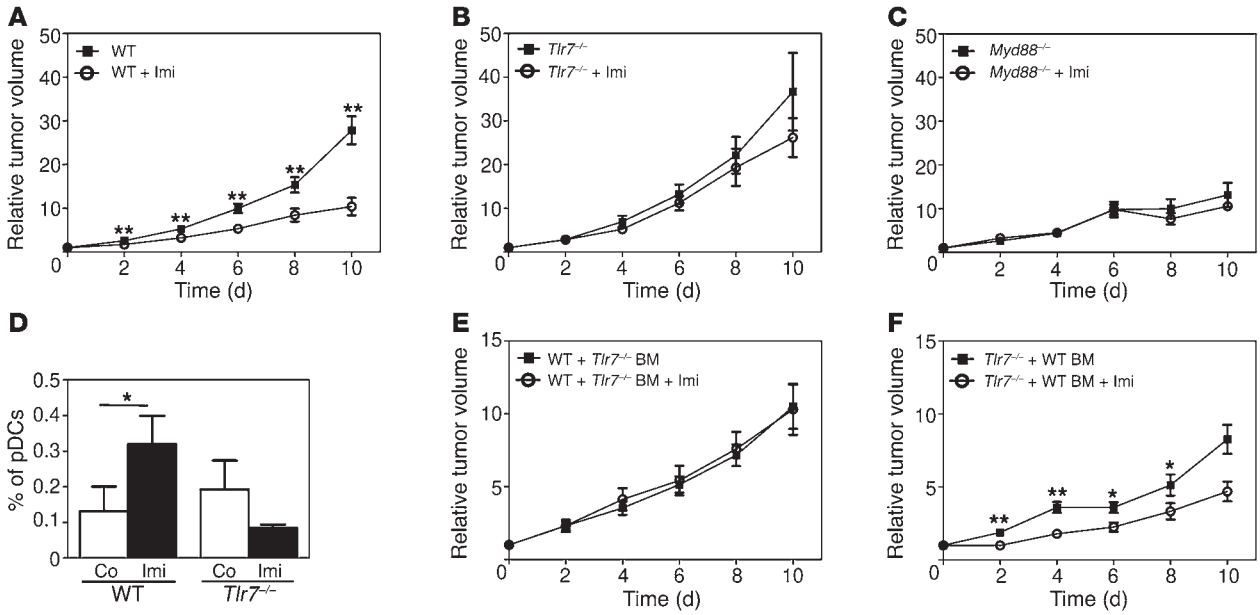

Figure 3

The antitumor effect of Imi depends on the presence of TLR7 and MyD88 on BM cells. (**A**–**C**) Graphs showing the kinetics of tumor growth in (**A**) C57BL/6 (WT), (**B**) *Tlr7*$^{-/-}$, and (**C**) *Myd88*$^{-/-}$ mice measured at the indicated time points after Imi treatment (n = 10–14 per group). (**D**) FACS analysis showing the percentage of pDCs (CD45$^+$CD11c$^+$B220$^+$CD11b$^-$) present in melanomas 3 days after Imi treatment. (**E** and **F**) Relative tumor volume in BM chimeras of the indicated genotypes after Imi treatment. C57BL/6 (WT) and *Tlr7*$^{-/-}$ mice were lethally irradiated and reconstituted intravenously with BM cells of the indicated genotypes. After 12 weeks, reconstituted mice were injected intradermally with B16-F10 melanoma cells, and tumors treated with Imi or left untreated (n = 7–11 per group). *$P < 0.05$, **$P < 0.005$.

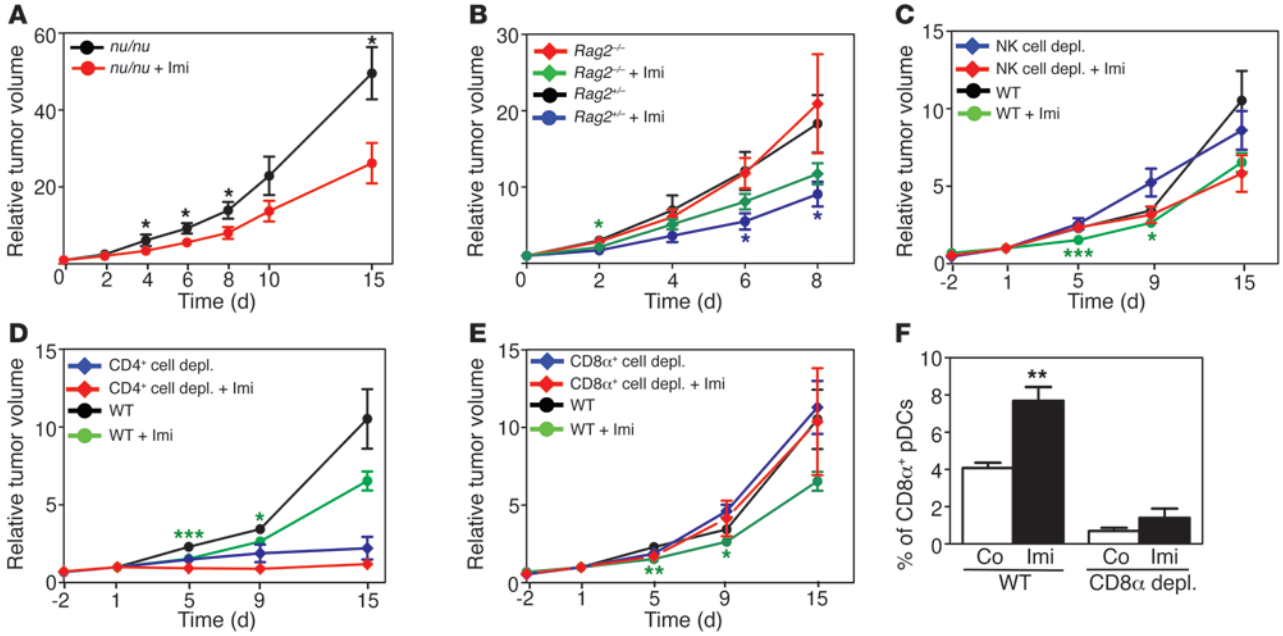

Figure 4

Adaptive immune cells are not required for the tumoricidal effect of Imi. (**A** and **B**) Graphs showing the relative tumor volume of (**A**) M3 melanomas intradermally induced in *Foxn1*^{nu} mice (*nu/nu* mice) and (**B**) B16-F10 melanomas induced in *Rag2*$^{-/-}$ and *Rag2*$^{+/-}$ mice as controls (n = 11–13 per group). (**C**–**E**) Relative tumor volume of M3 melanoma–bearing mice depleted of (**C**) NK cells by injection of anti-NK–specific antibodies (clone Asialo GM1); (**D**) CD4$^+$ cells by anti-CD4 antibody injection (clone GK1.5); or (**E**) CD8α$^+$ cells by anti-CD8α antibody injection (clone 53.6.7) before starting treatment with Imi (n = 8–9 per group). Untreated DBA/2 (WT) mice were used as controls. depl., depletion. (**F**) The percentage of CD8α$^+$ pDCs (CD11b$^-$B220$^+$) gated from CD45$^+$CD11c$^+$ cells present in melanomas of mice depleted of CD8α$^+$ cells 3 days after starting Imi treatment. *P < 0.05, **P < 0.005, ***P < 0.0005.

shown). Lack of TLR7, MyD88, or CCL2 also inhibited the infiltration of other immune cells after Imi application (Figure 2G and data not shown). These data demonstrate that CCL2 produced by mast cells in a TLR7/MyD88-dependent manner after Imi treatment is an important chemoattractant for pDCs and responsible for the inflammatory manifestations in the skin.

Imi induces a TLR7-dependent antitumor immune response. We have observed that tumor regression after Imi treatment correlates with the presence of increased numbers of pDCs in tumors (18). To determine the importance of TLR7 or MyD88 signaling for the antitumor response mediated by Imi, we used 2 orthotopic murine melanoma models, B16-F10 (C57BL/6) and M3 (DBA/2) melanoma cells, both of which induce aggressively growing tumors when injected intradermally in mice (Supplemental Figure 2A). As previously shown, Imi treatment of melanoma-bearing WT mice resulted in significantly reduced tumor growth (Figure 3A and ref. 18). However, the therapeutic effect of Imi was absent in mice lacking TLR7 or MyD88 (Figure 3, B and C). In WT mice, tumor-infiltrating pDCs were already observed 3 days after starting Imi treatment. In contrast, no increase in pDCs was observed in tumors of *Tlr7*$^{-/-}$ and *Myd88*$^{-/-}$ mice (Figure 3D and data not shown). To examine whether TLR7 and MyD88 expression is required on immune cells for tumor clearance, we reconstituted lethally irradiated WT mice with *Tlr7*$^{-/-}$ or *Myd88*$^{-/-}$ BM and *Tlr7*$^{-/-}$ or *Myd88*$^{-/-}$ mice with WT BM (Supplemental Figure 2B). BM reconstitution was confirmed by PCR before tumor induction (Supplemental Figure 3, C and D, and data not shown). In mice reconstituted with *Tlr7*$^{-/-}$ BM, tumors did not regress after Imi treatment (Figure 3E), whereas expression of TLR7 on BM cells was sufficient to restore the antitumor effect of Imi in a *Tlr7*$^{-/-}$ background (Figure 3F). Melanoma-bearing mice lacking MyD88 in BM-derived cells did not respond to Imi treatment, and Imi even slightly enhanced tumor growth (Supplemental Figure 2E). Surprisingly, *Myd88*$^{-/-}$ mice harboring WT BM-derived cells failed to respond to Imi, suggesting that MyD88-dependent proinflammatory signals might contribute to tumor growth (Supplemental Figure 2F and ref. 25). These results show that Imi-induced tumor clearance is dependent on TLR7 expression on BM-derived cells.

A CD8α-positive cell is responsible for the antitumor effect of Imi. Tumor infiltrates of WT mice treated with Imi contained increased numbers of activated CD8α$^+$ T cells and NK cells (Supplemental Figure 3A). However, the antitumor effect of Imi was not impaired in the absence of T cells, as melanomas grown in *Foxn1*^{nu} mice still responded to Imi treatment (Figure 4A). Similar results were obtained with tumors grown in *Rag2*$^{-/-}$ mice (Figure 4B). To investigate which leukocyte population is responsible for mediating tumor regression after Imi treatment, we performed antibody-mediated depletion of CD4$^+$, CD8α$^+$, and NK cells in melanoma-bearing mice. Mice with established tumors were injected with the respective antibodies before starting Imi treatment (Supplemental Figure 3B). Effective cell depletion in secondary lymphoid organs was confirmed by FACS analysis (Supplemental Figure 3, C and D). The composition of the infiltrating, remaining immune cells was comparable in tumors treated with antibodies or left untreated (data not shown). Notably, depletion of NK cells with 2 different antibodies (anti-AsialoGM1 and anti-NK1.1) did not affect the tumoricidal effect of Imi (Figure 4C and data not shown). These data suggest that B cells, cytotoxic T cells, NK cells, and, the recently described, IFN-producing killer DCs

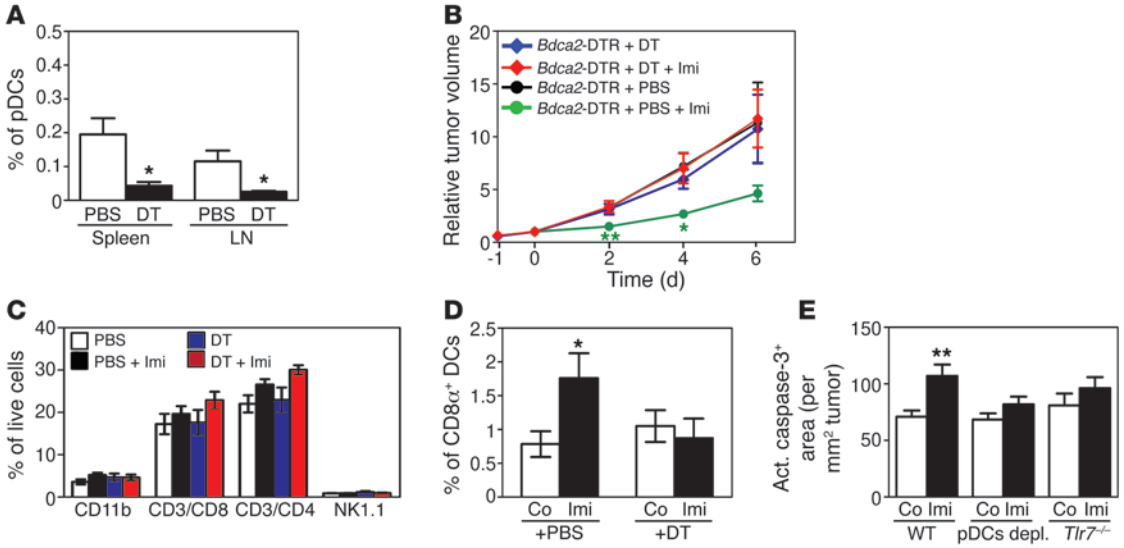

Figure 5

pDCs are responsible for the tumoricidal effect of Imi. (**A**) Graph demonstrating the absence of pDCs (CD11c$^+$B220$^+$SiglecH$^+$) in spleen and tumor draining lymph nodes of *Bdca2*-DTR mice depleted of pDCs by DT injection (+DT). Control (not pDC-depleted) mice were injected with PBS. (**B**) Relative tumor growth in pDC-depleted mice treated with Imi. *Bdca2*-DTR transgenic mice were depleted of pDCs prior to intradermal injection of B16-F10 cells (n = 5–7 per group). (**C** and **D**) FACS analysis showing the percentage of monocytes/neutrophils (CD11b$^+$), CD4$^+$ T cells (CD3$^+$CD4$^+$), CD8α$^+$ T cells (CD3$^+$CD8α$^+$), and NK cells (NK1.1$^+$) in (**C**) tumor-draining lymph nodes and (**D**) tumor-infiltrating CD8α$^+$ DCs in *Bdca2*-DTR mice treated as indicated. (**E**) Quantification of the active caspase-3–positive area (μm^2 per mm^2 of tumors) in tumor tissue of WT (n = 7–8 per group), pDC-depleted (pDCs depl.) (n = 8–9), and *Tlr7*$^{-/-}$ (n = 3) mice treated with Imi or left untreated. The active caspase-3$^+$ area was analyzed in 10 randomly chosen fields of at least 3 independent samples. *P < 0.05, **P < 0.005.

(IKDCs), which were described as NK1.1$^+$CD11c$^+$B220$^+$GR1$^-$ cells (26), do not play a major role in the antitumor immune response induced by Imi. Depletion of CD4$^+$ cells led to tumor stasis, which was not affected by Imi treatment (Figure 4D). Although Imi remained effective in tumor-bearing mice lacking T cells, in the absence of CD8α$^+$ cells, the antitumor response to Imi was entirely abolished (Figure 4E). To investigate which CD8α$^+$ cells other than cytotoxic T cells could be responsible for mediating the antitumor effect of Imi, we analyzed DC subpopulations in tumor-bearing mice. Within 3 days of Imi treatment we detected increased numbers of CD8α$^+$ pDCs in tumors, whereas, in CD8α$^+$-depleted mice, the number of CD8α$^+$ pDCs was dramatically reduced and did not increase after Imi treatment (Figure 4F). Similarly, pDCs isolated from spleen or cultured from BM displayed elevated CD8α levels in response to Imi treatment, which was dependent on TLR7 expression (Supplemental Figure 3, E and F, and data not shown). These data demonstrate that pDCs upregulate CD8α in a TLR7-dependent manner upon Imi stimulation and that these CD8α$^+$ pDCs might be important for the antitumor response of Imi.

pDCs mediate the antitumor effect of Imi in vivo. So far our data demonstrate that pDCs upregulate CD8α after Imi treatment and infiltrate into the tumor tissue by a TLR7-dependent mechanism. To determine whether pDCs are the mediators of the antitumor effect of Imi, we used *Bdca2*–diphtheria toxin receptor (*Bdca2*-DTR) transgenic mice expressing the DTR specifically in pDCs (27). Specific ablation of pDCs was obtained in tumor-bearing mice upon diphtheria toxin (DT) administration (Supplemental Figure 4A), as confirmed by FACS analysis of spleen and lymph nodes (Figure 5A and Supplemental Figure 4B). In melanoma-bearing mice depleted of pDCs, tumors did not regress after Imi treatment but kept growing like their untreated controls (Figure 5B). Lack of pDCs did not influence T cell, monocyte/neutrophil, and NK cell populations in tumors and tumor-draining lymph nodes of Imi-treated mice (Figure 5C and data not shown). Moreover, there was no increase of CD8α$^+$ DCs after Imi treatment in pDC-depleted mice (Figure 5D). Compared with that in WT mice, mice lacking TLR7 and pDC-depleted mice displayed reduced apoptosis in Imi-treated tumors, suggesting that TLR7-expressing pDCs were mediating this effect (Figure 5E and Supplemental Figure 4C). These data unequivocally show that pDCs and most likely CD8α$^+$ pDCs are essential for the antitumor effect of Imi.

Imi-activated pDCs induce tumor killing via cytolytic molecules. We next analyzed whether pDCs are able to directly kill tumor cells in response to Imi treatment. pDCs purified from Flt3L BM cultures or isolated ex vivo from BM were stimulated with Imi and cocultured with B16-F10 melanoma cells (Supplemental Figure 5A and data not shown). Both Imi-stimulated pDC populations showed increased cytotoxicity against melanoma cells compared with that of untreated controls (Figure 6A and data not shown). Imi-induced killing activity toward tumor cells was completely abolished when pDCs lacked TLR7 (Figure 6B), and there was no upregulation of CD8α on *Tlr7*$^{-/-}$ pDCs by Imi (Supplemental Figure 3F), suggesting that CD8α expression might be a prerequisite for the killing activity. To investigate whether killing was dependent on secreted cytotoxic molecules, melanoma cells were incubated with supernatants of Imi-stimulated pDCs. Supernatants from WT but not *Tlr7*$^{-/-}$ pDCs killed melanoma cells, indicating that soluble, death-inducing factors are produced by pDCs in a TLR7-dependent manner in response to Imi treatment (Figure 6C).

Next we investigated which cytolytic factors are produced by Imi-stimulated pDCs. It is known that TLR7 triggering on pDCs induces the production of IFN-α, which has been reported to

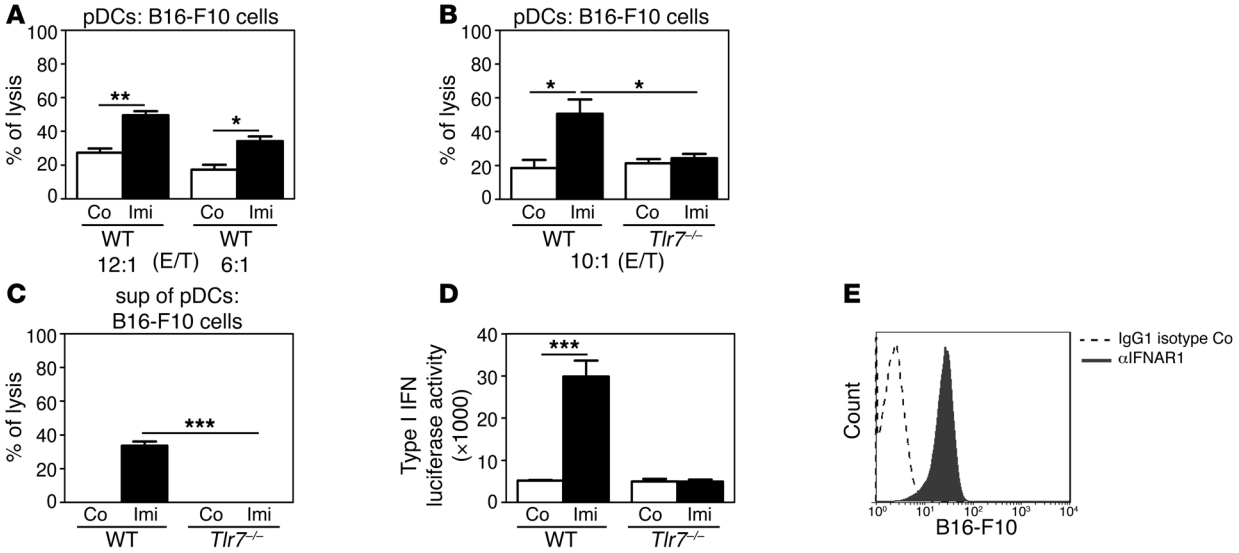

Figure 6

Imi-stimulated pDCs can directly kill tumor cells. (**A** and **B**) Killing assays measuring the percentage of lysis of B16-F10 melanoma cells occurring in pDCs that had been either (**A**) FACS sorted or (**B**) IMag sorted from Flt3L BM cultures of (**A**) WT and (**B**) *Tlr7*$^{-/-}$ mice and stimulated with Imi (2.5 μg/ml) for 16 hours. pDCs were cocultured with B16-F10 melanoma cells at indicated E/T ratios for 20 hours. (**C**) The killing assay was performed with the supernatant (sup) of the pDCs shown in **B**. (**D**) Type I IFN levels were determined by stimulating the IFN-luciferase reporter cell line LL171 (50) with supernatants of WT or *Tlr7*$^{-/-}$ pDCs triggered with Imi for 16 hours. (**E**) FACS analysis showing representative staining with anti-IFNAR1 antibodies (αIFNAR1) or isotype control (Co) rat IgG1 on B16-F10 cells. **P* < 0.05, ***P* < 0.005, ****P* < 0.0005.

induce apoptosis of tumor cells either directly (12, 28) or indirectly by stimulating death-receptor ligand expression (13, 14). In response to Imi, pDCs secreted high amounts of IFN-α, which could not be detected in pDCs lacking TLR7 (Figure 6D). Since B16-F10 melanoma cells express IFNAR1 on the cell surface, it is possible that they are directly killed by IFN-α/β (Figure 6E). However, antibody-mediated blocking of the IFNAR1 on melanoma cells could not prevent killing by pDCs, suggesting that other killing mechanisms are involved (data not shown).

We therefore investigated whether IFN-α/β induced by Imi can also indirectly kill tumor cells by inducing the production of death-receptor ligands in pDCs. These cytolytic molecules have been shown to be produced by T cells and NK cells as well as pDCs after IFNAR1 triggering (29–31). Since NK cells and T cells are not required for melanoma regression after Imi treatment (Figure 4, A–C), we analyzed whether Imi-triggered pDCs produce cytolytic molecules depending on TLR7 and IFNAR1 signaling. Imi treatment of pDCs significantly induced transcription and upregulation of *Trail*, which did not occur in pDCs from *Ifnar1*$^{-/-}$ and *Tlr7*$^{-/-}$ mice (Figure 7A and Supplemental Figure 5, B and C). Moreover, we found significantly elevated granzyme B levels in Imi-treated pDCs, which strictly depended on IFNAR1 and TLR7 expression (Figure 7B and Supplemental Figure 5D). Whereas perforin mRNA levels were not elevated in Imi-stimulated pDCs (data not shown), FasL expression was only moderately induced by Imi (Supplemental Figure 5E). In addition, TRAIL receptor 2 (DR5) was highly expressed on B16-F10 melanoma cells (Figure 7C), while only about 10% of melanoma cells expressed Fas receptor (Supplemental Figure 5F). A significant decrease of the cytotoxic capacity of Imi-stimulated pDCs and the supernatant thereof was observed (Figure 7, D and E) in the presence of the granzyme/perforin inhibitor ConcanamycinA (CMA) (32). Antibody-mediated blockade of TRAIL impaired pDC-induced killing after Imi treatment, which was, however, less efficient than the inhibition of granzyme B (Figure 7, F and G). Moreover, lysis of tumor cells could not be increased by the addition of recombinant TRAIL and was much less than that observed with supernatants of Imi-stimulated pDCs (Supplemental Figure 5G). These data demonstrate that pDCs can directly kill tumor cells in a TLR7- and IFNAR1-dependent manner, mainly by producing cytolytic molecules like granzyme B.

pDC-mediated tumor killing requires IFNAR1 signaling. To mechanistically define the role of IFNAR1 signaling in Imi-stimulated pDCs, we performed killing assays with *Ifnar1*$^{-/-}$ pDCs. Interestingly, Imi induced cytotoxicity of *Ifnar1*$^{-/-}$ pDCs and supernatants thereof was significantly decreased but not completely abolished (Figure 8, A and B). Similar results were also obtained by antibody-mediated inhibition of IFNAR1 on pDCs (Figure 8C). Interestingly, in Imi-stimulated *Ifnar1*$^{-/-}$ pDCs, upregulation of CD8α could still be observed in 50% of cells (Supplemental Figure 3F), providing a possible explanation for the incomplete blockade of the cytotoxic effects in the absence of IFNAR1 signaling. Moreover, in response to Imi treatment, *Ifnar1*$^{-/-}$ pDCs still produced high levels of type I IFNs (Figure 8D) as well as TNF-α (data not shown), which can also directly induce cell death (12, 28).

Next, we investigated whether the absence of IFNAR1 affects the Imi effects in vivo. Similar to that observed in *Tlr7*$^{-/-}$ *and Myd88*$^{-/-}$ mice (Figure 2C), levels of CCL2 were reduced in the dermis of *Ifnar1*$^{-/-}$ mice, and the number of pDCs did not increase upon Imi application (Figure 8, E and F). Melanoma grew slightly faster in *Ifnar1*$^{-/-}$ mice compared with that in WT mice, and Imi treatment did not show any tumoricidal effect (Figure 8G), presumably because there was no significant recruitment of pDCs into tumor tissue (Figure 8H). Our results

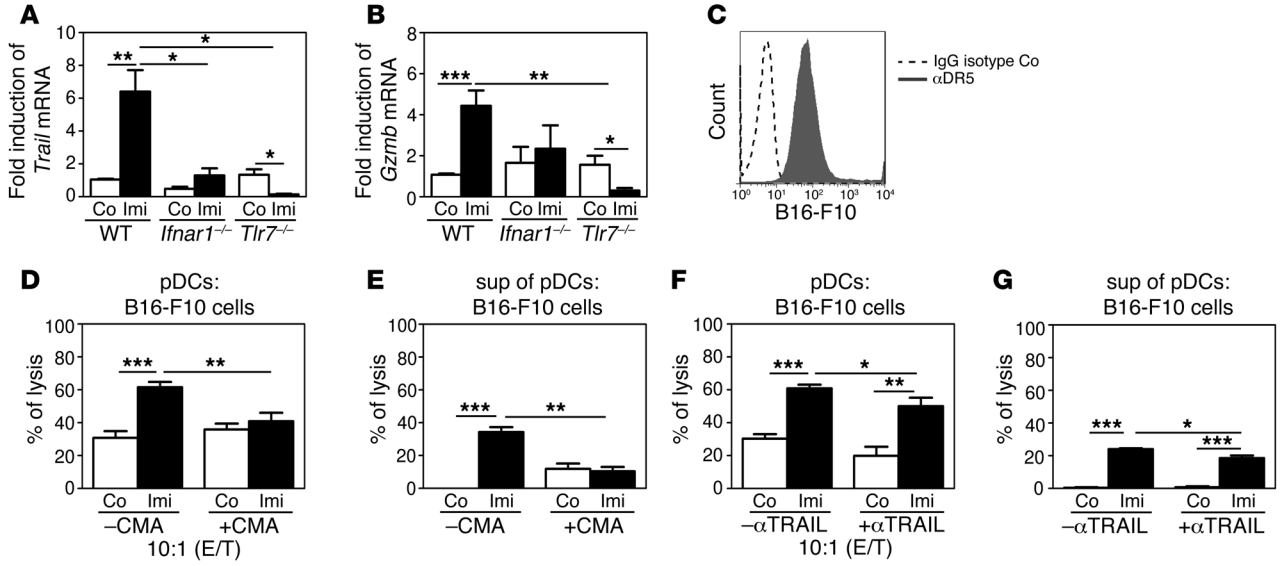

Figure 7

pDCs kill tumor cells via TRAIL and granzyme B. (**A** and **B**) qRT-PCR analysis for (**A**) *Trail* and (**B**) granzyme B (*Gzmb*) expression in IMag-sorted pDCs from Flt3L BM cultures of WT, *Ifnar1*$^{-/-}$, and *Tlr7*$^{-/-}$ mice stimulated for 6 hours with Imi (2.5 μg/ml). (**C**) FACS analysis showing DR5 expression on B16-F10 melanoma cells. (**D**–**G**) Killing assays performed with B16-F10 melanoma cells cocultured with (**D** and **F**) IMag-sorted pDCs from Flt3L cultures or (**E** and **G**) supernatants thereof previously treated with (**D** and **E**) 1 μg/ml CMA and 2.5 μg/ml Imi for 16 hours or with (**F** and **G**) anti-TRAIL antibody (αTRAIL) (25 μg/ml) for 2 hours and further stimulated with Imi (2.5 μg/ml) for 16 hours. Cytolytic assays were performed at a E/T ratio of 10:1. **P* < 0.05, ***P* < 0.005, ****P* < 0.0005.

demonstrate that IFNAR1 signaling is required, not only for tumor cell killing by pDCs, but also for CCL2 production and pDC recruitment after Imi treatment.

Discussion

The role of pDCs in tumors has long been under debate. Clinical studies have shown negative correlation between the numbers of infiltrating pDCs and patient prognosis (33). This was attributed to the finding that immature pDCs in tumors are weak inducers of T cell immunity or may even induce regulatory T cells (34, 35). In the present study, we demonstrate what we believe to be a novel function for pDCs as active and indispensable effectors of tumor killing after treatment with Imi. Moreover, we show that TLR7 and IFNAR1 signaling in pDCs is necessary for tumor killing upon Imi treatment.

We observed increased CCL2 levels in the dermis shortly after Imi stimulation, which was dependent on TLR7, MyD88, and IFNAR1 expression. Consistently, pDC recruitment to the dermis and tumors after Imi treatment was dramatically impaired, and the inflammatory response in the dermis was much weaker in these knockout mice. Mice deficient for CCL2 did not show increased numbers of pDCs in the skin after Imi application, thus providing strong evidence that CCL2 is necessary for pDC recruitment. Our results with BM-reconstituted mice demonstrate that Imi is still effective when TLR7 is missing in dermal cells of non-BM origin and that the tumoricidal effect of Imi strictly requires TLR7 expression on BM-derived cells. Since TLR7 signaling is required for CCL2 production, these results strongly suggest that a skin-resident, TLR7-expressing BM-derived cell is responsible for CCL2 production after Imi treatment. Dermal mast cells are strong candidates, as they express TLR7 and produce cytokines upon Imi treatment (24). Recent studies have also shown that mast cells can produce CCL2 after anti-IgE stimulation (36). We observed that mast cells produced significant amounts of CCL2 after Imi treatment, therefore strengthening our hypothesis that mast cells are responsible for CCL2 production and subsequent pDC recruitment after topical Imi application.

Although we found increased apoptosis and activation of the MAPK pathway in Imi-treated primary keratinocytes isolated from *Tlr7*$^{-/-}$ and *Myd88*$^{-/-}$ mice, it is evident from our results that Imi-induced epidermal apoptosis does not significantly contribute to local inflammation and pDC infiltration. Imi can also directly induce apoptosis of melanoma cells. However, this alone is not sufficient for tumor resolution, since tumor regression is strictly dependent on the presence of pDCs. Imi loses its therapeutic effect in *Tlr7*$^{-/-}$, *Myd88*$^{-/-}$, and *Ifnar1*$^{-/-}$ mice. This is accompanied by reduction of CCL2 expression and tumor-infiltrating pDCs. TLR9-activated pDCs induce NK cell– and CD8$^+$ T cell–mediated antitumor immunity by driving maturation of and cross-presentation by conventional DCs (22). Although T cell and NK cell activity can be modulated by TLR7 agonists (37, 38), we show that the antitumor response induced by Imi remained effective, even in the absence of T and NK cells and IKDCs.

We provide definitive proof that pDCs are essential for Imi-induced tumor killing by depleting pDCs in tumor-bearing *Bdca2*-DTR transgenic mice (9). Lack of pDCs completely abolished the tumoricidal effect of Imi in these mice but did not influence other immune cell populations, emphasizing the central role for pDCs in the antitumor response induced by Imi. In vivo depletion of CD8α$^+$ cells also abolished the tumoricidal effect of Imi, similar to that in pDC-depleted mice. Naive pDCs have been shown to express variable amounts of CD8α on their surface, and we show that Imi treatment induces TLR7-dependent upregulation of CD8α on pDCs in vivo and in vitro. Importantly, in vivo depletion of CD8α$^+$ cells also ablated activated pDCs from tumors, providing an explanation for why Imi treatment was not active in mice lacking CD8α$^+$ cells.

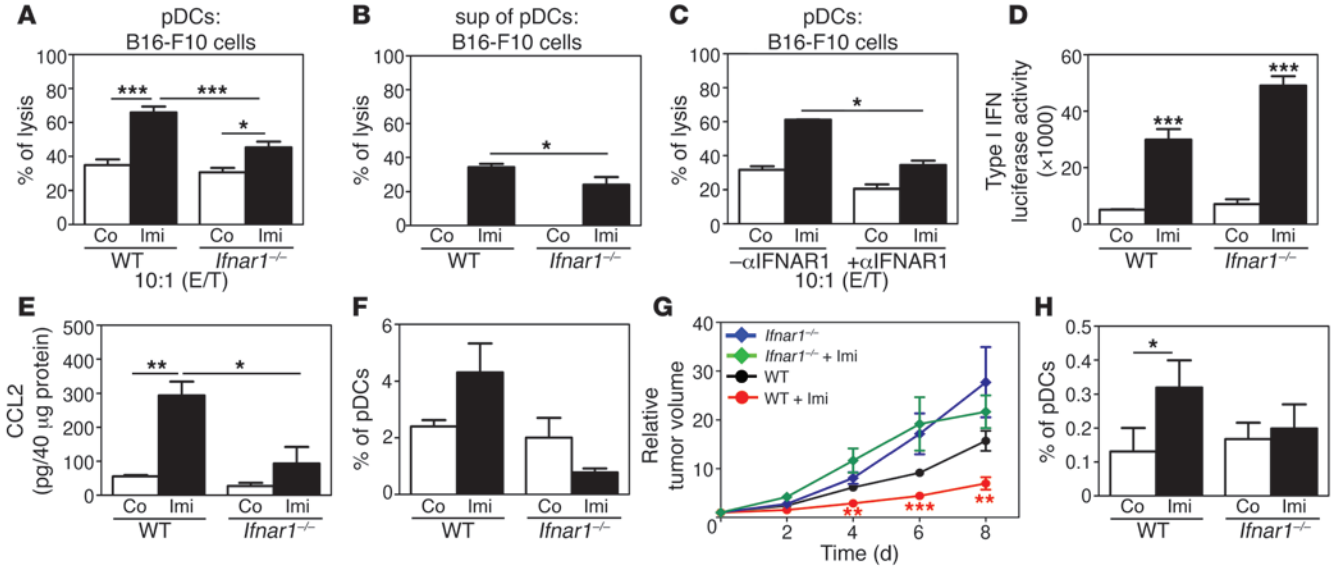

Figure 8

pDCs require IFNAR1 signaling for their cytotoxic activity. (**A** and **B**) Killing assay performed with B16-F10 melanoma cells cocultured with (**A**) IMag-sorted WT or *Ifnar1*$^{-/-}$ pDCs or (**B**) supernatants thereof. (**C**) Killing assay with pDCs pretreated with anti-IFNAR1 antibody (25 μg/ml) and simulated with Imi for 16 hours before coculturing with B16-F10 cells. Cytolytic assays were performed at a E/T ratio of 10:1. (**D**) Type I IFN levels were analyzed by culturing the IFN-luciferase reporter cell line LL171 with supernatants of WT or *Ifnar1*$^{-/-}$ pDCs that had been stimulated with Imi for 16 hours. (**E**) CCL2 levels measured in dermal protein lysates by ELISA after WT and *Ifnar1*$^{-/-}$ mouse back skin was treated for 24 hours with Imi or left untreated. (**F**) Graph showing the percentage of B220^{+}Ly6C^{+}CD11b^{-} pDCs among total CD45^{+}CD11c^{+} DCs in the dermis after 7 days of topical Imi treatment. (**G**) Growth of intradermally injected B16-F10 melanomas in WT and *Ifnar1*$^{-/-}$ mice after Imi treatment (n = 8–9 mice per group). (**H**) FACS analysis showing the percentage of pDCs (CD45^{+}CD11c^{+}B220^{+}CD11b^{-}) infiltrating into melanomas shown in **G** on day 3. *P < 0.05, **P < 0.005, ***P < 0.0005.

In response to TLR7, triggering pDCs can produce high amounts of type I IFN (4, 11), which can influence tumor growth by stimulating the adaptive immune system or by activating innate immune responses (9, 12, 14). IFNAR1 knockout mice are impaired in their ability to induce adaptive immune responses in response to TLR7 ligation by the synthetic agonist polyUs21 (39). Moreover, it has been shown that IFN-α/β can directly contribute to the clearance of tumor cells in a caspase-dependent manner (12, 28) or indirectly contribute by the upregulation of cytotoxic molecules (13, 14). We did not observe direct killing of tumor cells by IFN-α/β, as inhibition of IFNAR1 on tumor cells did not prevent killing induced by Imi-stimulated pDCs. Therefore, it is likely that IFN-α/β stimulates death receptor ligand expression in pDCs. Human pDCs have been implicated in exertion of cytolytic functions by upregulating TRAIL (17) or influencing T cell responses by granzyme B secretion (40). Furthermore, human pDCs have been shown to partially inhibit proliferation of a melanoma cell line in a type I IFN-dependent manner (41).

A number of molecules responsible for tumor cell killing, like granzyme B, TRAIL, FasL, and TNF-α, were upregulated in Imi-stimulated pDCs, although to a variable degree. However, analysis of these factors was hampered by the fact that they may be stored and released within microvesicles or shed from the surface (42). Expression of these lytic molecules was dependent on TLR7 expression and on IFNAR1 signaling in pDCs. Imi treatment did not lead to tumor clearance in *Ifnar1*$^{-/-}$ mice, and Imi-induced cytotoxicity of *Ifnar1*$^{-/-}$ pDCs toward melanoma cells was significantly reduced. Blocking of granzyme B led to a significant decrease of melanoma cell death by Imi-stimulated pDCs, providing strong evidence that the killing activity of pDCs is primarily mediated by granzyme B. TRAIL and FasL were both expressed only in a subpopulation of pDCs; however, their expression was only minimally overlapping (data not shown). In vitro blocking of TRAIL/DR5 significantly reduced tumor cell lysis, but it did not entirely inhibit killing, suggesting that TRAIL only partially contributes to the in vivo effect of Imi. Although pDCs do not produce perforin, which is thought to be essential for the delivery of granzyme B into the cytosol, it is still under debate whether pDCs are able to induce cell death via granzyme B alone. Evidence is growing that perforin-independent mechanisms also induce the uptake of granzyme B to induce killing of tumor cells (43). It is therefore tempting to speculate that Imi could replace the requirement for perforin for granzyme B uptake by tumor cells.

Based on our results, we propose that topical application of Imi leads to skin inflammation via TLR7/MyD88-dependent and -independent mechanisms. Imi-stimulated keratinocytes show increased apoptosis, which is independent of TLR7/MyD88-signaling. Instead, Imi-induced CCL2 production by resident mast cells and subsequent pDC recruitment into skin and tumors is strictly dependent on TLR7/MyD88 and IFNAR1 expression. Once pDCs are recruited to the skin or tumors, Imi stimulation leads to TLR7-dependent upregulation of type I IFNs, which in turn act in an autocrine manner on pDCs and induce the secretion of cytolytic molecules like TRAIL and granzyme B via IFNAR1 signaling (Figure 9). In mice lacking TLR7/MyD88 and IFNAR1, there is no induction of CCL2 and, as a consequence, no recruitment of pDCs and also no upregulation of cytolytic molecules, providing an explanation for the lack of therapeutic effect of Imi in these knockout mice. In conclusion, our data provide a very

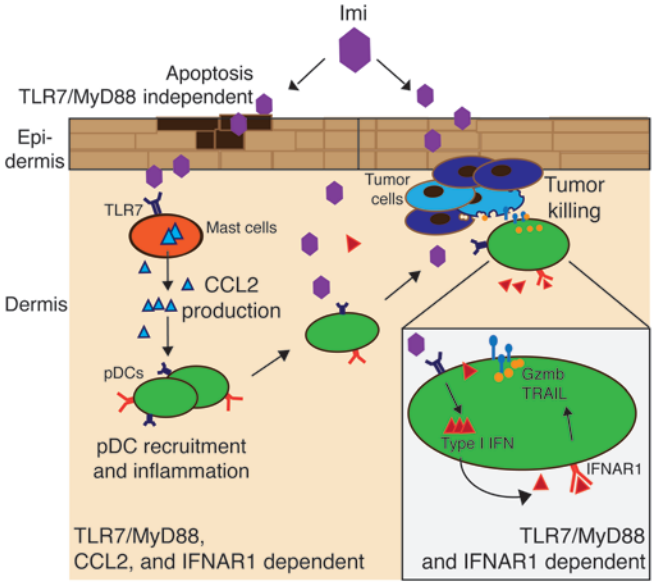

Figure 9
Mechanism of Imi-mediated tumor cell killing by pDCs. Topical Imi treatment leads to increased apoptosis in keratinocytes independently of TLR7 and MyD88. Dermal mast cells secrete CCL2 after Imi stimulation in a TLR7/MyD88- and IFNAR1-dependent manner, resulting in skin inflammation and recruitment of pDCs to the treated sites. Imi-activated pDCs produce high amounts of type I IFNs, which act in an autocrine manner on pDCs to upregulate cytolytic molecules like granzyme B (*Gzmb*) and TRAIL via IFNAR1 signaling, thereby transforming pDCs into a subset of killer DCs able to directly eliminate tumor cells.

strong demonstration that pDCs are absolutely required for the antitumor response mediated by Imi. Therefore, strategies aiming at promoting the recruitment of pDCs to tumor sites and reprogramming them to become killer pDCs might prove to be effective stand-alone or adjuvant antitumor therapies.

Methods

Mice, cells, and tumor induction. C57BL/6, DBA/2, and *Foxn1*^{nu} were purchased from Harlan Laboratories. *Rag2*$^{-/-}$ (44), *Ifnar1*$^{-/-}$ (45), *Myd88*$^{-/-}$ (46), *Tlr7*$^{-/-}$ (4), *Ccl2*$^{-/-}$ (47), and *Bdca2*-DTR mice (9) were kept in the animal facility of the Medical University of Vienna. Melanoma cells, M3 of H-2^{d} haplotype (derived from Cloudman S91 melanoma; H-2^{d}), were cultured as previously described (18). B16-F10 melanoma cells of C57BL/6 background (H-2^{b}) were cultured in MEM (PAA) in the presence of 10% FCS (PAA), 1% penicillin and streptomycin (Pen/Strep) (PAA), and 1% HCO_3. Orthotopic tumors (melanomas) were induced in waxed back skin of DBA/2 or C57BL/6 mice by intradermal injection of M3 (1×10^6) or B16-F10 melanoma cells (3.5×10^4), as previously described (18). Tumors were treated topically with Aldara, a 5% Imi cream formulation, every other day or left untreated. Tumors were measured with a caliper by determining the greatest longitudinal and transverse diameters (length and width). Tumor volume was calculated by using the ellipsoidal formula, $\pi/6 \times (\text{length} \times \text{width})^2$. The relative tumor volume for each time point represents the ratio between the measured volume and the volume at time 0 (start of Imi treatment). For in vitro studies, Imi (Invivogen) was dissolved in endotoxin-free Limulus amebocyte lysate (LAL) water.

Cell depletion experiments in vivo. For in vivo cell depletion experiments, antibodies against CD4 (clone GK1.5, rat IgG2bK) and CD8α (clone 53.6.7, rat [Lou/Ws1/M] IgG2aK) were isolated from hybridoma supernatants and injected i.p. at a dose of 0.5 mg/mouse every 5 days. For depletion of NK cells, 0.5 mg anti–asialo-GM1 antibody (Rabbit IgG, WAKO, Japan) or anti-NK1.1 were injected once a week. Antibodies or the respective isotype control were injected when tumors were visible. Imi treatment was started 2 days later and repeated every other day. Depletion efficiency was determined in peripheral blood 4 days after antibody injection and in tumors and tumor-draining lymph nodes at the end of the experiment. In vivo depletion of pDCs was induced by DT injection (i.p.; 4.5 ng DT/g body weight every other day) in *Bdca2*-DTR mice harboring B16-F10 melanoma cells 1 day before the start of Imi treatment.

Dermal and epidermal cell cultures and Western blot analysis. Epidermal cells were isolated and cultured on vitrogen/fibronectin-coated dishes in low-calcium MEM-medium (Sigma-Aldrich) containing 8%-chelated FCS for 4 to 5 days, as previously described (48). Dermal cells were isolated as previously described (49) and cultured in MEM medium (PAA) containing 10% FCS at 37°C and 5% CO_2. Cells were treated with soluble Imi (12 μg/ml; Invivogen) for the indicated time points (see Figure 1 and Supplemental Figure 1). Western blot analysis was performed as previously described (48) with antibodies detecting phospho-JNK (Cell Signaling Technology), JNK (Cell Signaling Technology), phospho-p38 (Cell Signaling Technology), p38 (Cell Signaling Technology), phospho-p44/42 (Cell Signaling Technology), and ERK1/ERK2 (Santa Cruz Biotechnology).

Flow cytometric analysis. Dissected tumors were incubated with Liberase (Roche) for 60 minutes at 37°C. After red blood cell lysis, the cell suspension was stained with the indicated mAbs (see the legends for Figures 3–5 and 8) for 30 minutes at 4°C. Dermal and epidermal cell suspensions were isolated and stained with fluorescently labeled antibodies after blocking with Fc-block (BD Pharmingen). The following mAbs were used: anti–Annexin V (BD Pharmingen), anti-CD11b (Biolegend), anti-CD11c (Biolegend, BD Pharmingen), anti-CD45 (Biolegend), anti-B220 (Biolegend), anti-CD8α (Biolegend), anti-mPDCA1 (Miltenyi Biotec), anti–Gr-1 (Biolegend), anti-Ly6C (Biolegend), anti-CD4 (BD Pharmingen), anti-CD49b (BD Pharmingen), anti-NK1.1 (Biolegend), anti-CD3 (BD Pharmingen), anti-I-A/I-E (MHCII, Biolegend), anti-TRAIL (Biolegend), anti-FasL (Biolegend), anti–IFNAR-1 (Biolegend), anti-Fas (BD Pharmingen), and anti–DR5 (Biolegend). Before staining with intracellular anti–granzyme B (clone 16G6, eBioscience), cells were cultured in presence of GolgiPlug (BD Biosciences) for 4 hours. Data were acquired on a FACSCalibur or LSR-II Flow Cytometer (BD Biosciences) and analyzed using CellQuest software (BD Biosciences) or FlowJo (Treestar).

ELISA and luciferase assay. Mouse IL-6 (R&D Systems), TNF-α (BD Biosciences), IL-1β (BD Biosciences), or CCL2 (BD Biosciences) immunoassays were performed according to manufacturer's instructions, with supernatants collected from cell cultures or with 40 μg of protein lysates. LL171 cells were used for type I IFN measurement in supernatants of BM-derived pDCs, as previously described (50). Luciferase activity was measured with Beetle Luciferin, Potassium Salt (Promega) using a Mithras Microplate reader.

Immunofluorescence analysis. Cryosections from mouse tissue and epidermal ear sheets were prepared as previously described (49). Five-micron sections were stained with H&E (Sigma-Aldrich) according to standard procedures. Immunofluorescence stainings were performed with an anti-mouse active caspase-3 (R&D systems) antibody and secondary antibodies purchased from Molecular Probes and Vector Laboratories.

Total RNA isolation and RT-PCR analysis. Total RNA from tissues and cells was isolated with TRIzol Reagent (Invitrogen). cDNA synthesis was performed with the SuperScript First-Strand Synthesis System (Invitrogen) according to the manufacturer's instructions. RT-PCR was performed with primers for TLR1–TLR9, TLR11, and GAPDH (Supplemental Table 1). qRT-PCR reactions were carried out using SYBR Green Mix (Applied Biosystems), according to the manufacturer's instructions, with primers detecting actin, TRAIL, and Gzmb (Supplemental Table 1).

BM cultures and cytolytic assays. BM was isolated from mice by flushing the tibiae and femurs with RPMI-1640 (Gibco). BM-derived mast cells were obtained by culturing BM cells in RPMI supplemented with 10% FCS, 1% Pen/Strep, β-mercaptoethanol, and 5 ng/ml IL-3 (R&D Systems) for 5 weeks (purity was routinely > 94%). BM-derived pDCs were obtained by differentiating BM cells in RPMI supplemented with 10% FCS, 1% Pen/Strep, nonessential amino acids, sodium pyruvate, β-mercaptoethanol, and 80 ng/ml Flt3L (R&D Systems) for 8 days. Cytolytic assays were performed as described elsewhere (51). Briefly, pDCs from Flt3L BM cultures were sorted for $B220^+CD11b^-$ cells either by FACS (purity was routinely >93%) or IMag-Streptavidin beads (BD Biosciences) (purity was routinely >80%) and stimulated with Imi (2.5 μg/ml) for 16 hours. B16-F10 cells (0.5×10^4) were seeded for 4 hours before adding stimulated pDCs at the indicated effector-to-target cell (E/T) ratios and cocultured for 20 hours. The percentage of tumor cell lysis was comparable between FACS- and IMag-purified pDCs. Experiments were also performed in presence of SuperKillerTRAIL (Enzo Life Sciences) or neutralizing antibodies against mouse TRAIL (Biolegend), mouse IFNAR1 (clone MAR1-5A3, Biolegend), and CMA (Sigma-Aldrich). Cytotoxicity was measured in 96-well plates using EZ4U nonradioactive cell proliferation and cytotoxicity assay (Biomedica) according to the manufacturer's manual. Data were expressed as the percentage of cytotoxicity, calculated by the following formula: % lysis = $(1 - (A_{\text{of cocultured cells}} - A_{\text{of effector cells}})/A_{\text{of target cells}}) \times 100$, where A stands for absorbance.

Statistics. Data were analyzed by 2-tailed Student's, Mann-Whitney, or Wilcoxon-matched paired test. Error bars represent ± SEM of at least 2 independent experiments, unless otherwise stated. P values of less than 0.05 were considered statistically significant.

Study approval. Mice were kept in the animal facility of the Medical University of Vienna in accordance with institutional policies and federal guidelines. Animal experiments were approved by the Animal Experimental Ethics Committee of the Medical University of Vienna and the Austrian Federal Ministry of Science and Research.

Acknowledgments

We are thankful to Christine Chou for the NK cell depletion experiment and Elisabeth Moser and Stefanie Wculek for experimental help. We thank Mathias Müller for providing the *Ifnar1*$^{-/-}$ mice and Shizuo Akira and Caetano Reis e Sousa for providing the *Tlr7*$^{-/-}$ and *Myd88*$^{-/-}$ mice of C57BL/6 background. We are grateful to Thomas Decker and Johannes Stöckl for critical reading of the manuscript. This work was supported by the following Austrian Science Fund (FWF) grants: Special Research Program SFB-23-B13 and the doctoral program "Inflammation and Immunity" DK W1212 and P18782. M. Sibilia acknowledges funding from the EC program LSHC-CT-2006-037731 (Growthstop) and the Austrian Federal Government's GEN-AU program "Austromouse" (GZ 200.147/1-VI/1a/2006 and 820966). B. Drobits was the recipient of a DOC-Forte PhD fellowship from the Austrian Academy of Sciences.

Received for publication September 15, 2011, and accepted in revised form December 7, 2011.

Address correspondence to: Maria Sibilia, Institute for Cancer Research, Department of Medicine I, Comprehensive Cancer Center, Medical University of Vienna, Borschkegasse 8a, 1090 Vienna, Austria. Phone: 43.1.4277.65131; Fax: 43.1.4277.65193; E-mail: maria.sibilia@meduniwien.ac.at.

Roland Grundtner's present address is: Bristol-Myers Squibb GesmbH, Vienna, Austria.

1. Smits EL, Ponsaerts P, Berneman ZN, Van Tendeloo VF. The use of TLR7 and TLR8 ligands for the enhancement of cancer immunotherapy. *Oncologist*. 2008;13(8):859–875.
2. Li VW, Li WW, Talcott KE, Zhai AW. Imiquimod as an antiangiogenic agent. *J Drugs Dermatol*. 2005; 4(6):708–717.
3. Schon MP, et al. Death receptor-independent apoptosis in malignant melanoma induced by the small-molecule immune response modifier imiquimod. *J Invest Dermatol*. 2004;122(5):1266–1276.
4. Hemmi H, et al. Small anti-viral compounds activate immune cells via the TLR7 MyD88-dependent signaling pathway. *Nat Immunol*. 2002;3(2):196–200.
5. Diebold SS, Kaisho T, Hemmi H, Akira S, Reis e Sousa C. Innate antiviral responses by means of TLR7-mediated recognition of single-stranded RNA. *Science*. 2004;303(5663):1529–1531.
6. Schon MP, Schon M, Klotz KN. The small antitumoral immune response modifier imiquimod interacts with adenosine receptor signaling in a TLR7- and TLR8-independent fashion. *J Invest Dermatol*. 2006;126(6):1338–1347.
7. Kanneganti TD, et al. Bacterial RNA and small antiviral compounds activate caspase-1 through cryopyrin/Nalp3. *Nature*. 2006;440(7081):233–236.
8. Akira S, Takeda K. Toll-like receptor signalling. *Nat Rev Immunol*. 2004;4(7):499–511.
9. Swiecki M, Colonna M. Unraveling the functions of plasmacytoid dendritic cells during viral infections, autoimmunity, and tolerance. *Immunol Rev*. 2010;234(1):142–162.
10. Asselin-Paturel C, et al. Type I interferon dependence of plasmacytoid dendritic cell activation and migration. *J Exp Med*. 2005;201(7):1157–1167.
11. Gibson SJ, et al. Plasmacytoid dendritic cells produce cytokines and mature in response to the TLR7 agonists, imiquimod and resiquimod. *Cell Immunol*. 2002;218(1–2):74–86.
12. Thyrell L, et al. Mechanisms of Interferon-alpha induced apoptosis in malignant cells. *Oncogene*. 2002;21(8):1251–1262.
13. Papageorgiou A, Dinney CP, McConkey DJ. Interferon-alpha induces TRAIL expression and cell death via an IRF-1-dependent mechanism in human bladder cancer cells. *Cancer Biol Ther*. 2007; 6(6):872–879.
14. Herzer K, et al. IFN-alpha-induced apoptosis in hepatocellular carcinoma involves promyelocytic leukemia protein and TRAIL independently of p53. *Cancer Res*. 2009;69(3):855–862.
15. Chaperot L, et al. Virus or TLR agonists induce TRAIL-mediated cytotoxic activity of plasmacytoid dendritic cells. *J Immunol*. 2006;176(1):248–255.
16. Colisson R, et al. Free HTLV-1 induces TLR7-dependent innate immune response and TRAIL relocalization in killer plasmacytoid dendritic cells. *Blood*. 2009;115(11):2177–2185.
17. Stary G, Bangert C, Tauber M, Strohal R, Kopp T, Stingl G. Tumoricidal activity of TLR7/8-activated inflammatory dendritic cells. *J Exp Med*. 2007; 204(6):1441–1451.
18. Palamara F, Meindl S, Holcmann M, Luhrs P, Stingl G, Sibilia M. Identification and characterization of pDC-like cells in normal mouse skin and melanomas treated with imiquimod. *J Immunol*. 2004;173(5):3051–3061.
19. Schiller M, Metze D, Luger TA, Grabbe S, Gunzer M. Immune response modifiers--mode of action. *Exp Dermatol*. 2006;15(5):331–341.
20. Penna G, Vulcano M, Sozzani S, Adorini L. Differential migration behavior and chemokine production by myeloid and plasmacytoid dendritic cells. *Hum Immunol*. 2002;63(12):1164–1171.
21. Vermi W, Soncini M, Melocchi L, Sozzani S, Facchetti F. Plasmacytoid dendritic cells and cancer. *J Leukoc Biol*. 2011;90(4):681–690.
22. Liu C, et al. Plasmacytoid dendritic cells induce NK cell-dependent, tumor antigen-specific T cell cross-priming and tumor regression in mice. *J Clin Invest*. 2008; 118(3):1165–1175.
23. Sorrentino R, et al. Plasmacytoid dendritic cells alter the antitumor activity of CpG-oligodeoxynucleotides in a mouse model of lung carcinoma. *J Immunol*. 2010;185(8):4641–4650.
24. Heib V, et al. Mast cells are crucial for early inflammation, migration of Langerhans cells, and CTL responses following topical application of TLR7 ligand in mice. *Blood*. 2007;110(3):946–953.
25. Rakoff-Nahoum S, Medzhitov R. Regulation of spontaneous intestinal tumorigenesis through the adaptor protein MyD88. *Science*. 2007; 317(5834):124–127.
26. Taieb J, et al. A novel dendritic cell subset involved in tumor immunosurveillance. *Nat Med*. 2006; 12(2):214–219.
27. Swiecki M, Gilfillan S, Vermi W, Wang Y, Colonna M. Plasmacytoid dendritic cell ablation impacts early interferon responses and antiviral NK and CD8(+) T cell accrual. *Immunity*. 2010;33(6):955–966.
28. Liu ZG. Molecular mechanism of TNF signaling and beyond. *Cell Res*. 2005;15(1):24–27.
29. Sato K, et al. Antiviral response by natural killer cells through TRAIL gene induction by IFN-alpha/beta. *Eur J Immunol*. 2001;31(11):3138–3146.
30. Kohlmeier JE, Cookenham T, Roberts AD, Miller SC, Woodland DL. Type I interferons regulate cytolytic activity of memory CD8(+) T cells in the lung airways during respiratory virus challenge. *Immunity*. 2010;33(1):96–105.
31. Stary G, et al. Plasmacytoid dendritic cells express

TRAIL and induce CD4+ T-cell apoptosis in HIV-1 viremic patients. *Blood*. 2009;114(18):3854–3863.
32. Shinbori T, Walczak H, Krammer PH. Activated T killer cells induce apoptosis in lung epithelial cells and the release of pro-inflammatory cytokine TNF-alpha. *Eur J Immunol*. 2004;34(6):1762–1770.
33. Treilleux I, et al. Dendritic cell infiltration and prognosis of early stage breast cancer. *Clin Cancer Res*. 2004;10(22):7466–7474.
34. Zou W, et al. Stromal-derived factor-1 in human tumors recruits and alters the function of plasmacytoid precursor dendritic cells. *Nat Med*. 2001; 7(12):1339–1346.
35. Wei S, et al. Plasmacytoid dendritic cells induce CD8+ regulatory T cells in human ovarian carcinoma. *Cancer Res*. 2005;65(12):5020–5026.
36. Kato A, et al. Dexamethasone and FK506 inhibit expression of distinct subsets of chemokines in human mast cells. *J Immunol*. 2009; 182(11):7233–7243.
37. Sawaki J, et al. Type 1 cytokine/chemokine production by mouse NK cells following activation of their TLR/MyD88-mediated pathways. *Int Immunol*. 2007; 19(3):311–320.
38. Ooi T, et al. Imiquimod-induced regression of actinic keratosis is associated with infiltration by T lymphocytes and dendritic cells: a randomized controlled trial. *Br J Dermatol*. 2006;154(1):72–78.
39. Rajagopal D, Paturel C, Morel Y, Uematsu S, Akira S, Diebold SS. Plasmacytoid dendritic cell-derived type I interferon is crucial for the adjuvant activity of Toll-like receptor 7 agonists. *Blood*. 2010; 115(10):1949–1957.
40. Jahrsdorfer B, et al. Granzyme B produced by human plasmacytoid dendritic cells suppresses T-cell expansion. *Blood*. 2009;115(6):1156–1165.
41. Inglefield JR, et al. TLR7 agonist 852A inhibition of tumor cell proliferation is dependent on plasmacytoid dendritic cells and type I IFN. *J Interferon Cytokine Res*. 2008;28(4):253–263.
42. Monleon I, et al. Differential secretion of Fas ligand- or APO2 ligand/TNF-related apoptosis-inducing ligand-carrying microvesicles during activation-induced death of human T cells. *J Immunol*. 2001; 167(12):6736–6744.
43. Gross C, Koelch W, DeMaio A, Arispe N, Multhoff G. Cell surface-bound heat shock protein 70 (Hsp70) mediates perforin-independent apoptosis by specific binding and uptake of granzyme B. *J Biol Chem*. 2003;278(42):41173–41181.
44. Shinkai Y, et al. RAG-2-deficient mice lack mature lymphocytes owing to inability to initiate V(D)J rearrangement. *Cell*. 1992;68(5):855–867.
45. Muller U, et al. Functional role of type I and type II interferons in antiviral defense. *Science*. 1994; 264(5167):1918–1921.
46. Adachi O, et al. Targeted disruption of the MyD88 gene results in loss of IL-1- and IL-18-mediated function. *Immunity*. 1998;9(1):143–150.
47. Lu B, et al. Abnormalities in monocyte recruitment and cytokine expression in monocyte chemoattractant protein 1-deficient mice. *J Exp Med*. 1998;187(4):601–608.
48. Lichtenberger BM, Tan PK, Niederleithner H, Ferrara N, Petzelbauer P, Sibilia M. Autocrine VEGF signaling synergizes with EGFR in tumor cells to promote epithelial cancer development. *Cell*. 2010; 140(2):268–279.
49. Holcmann M, et al. Skin inflammation is not sufficient to break tolerance induced against a novel antigen. *J Immunol*. 2009;183(2):1133–1143.
50. Uze G, et al. Domains of interaction between alpha interferon and its receptor components. *J Mol Biol*. 1994;243(2):245–257.
51. Ma F, Zhang J, Zhang C. The TLR7 agonists imiquimod and gardiquimod improve DC-based immunotherapy for melanoma in mice. *Cell Mol Immunol*. 2010;7(5):381–388.